Visual Augmentation for Personal Air Vehicles During Flight Control System Degradation

Tim Mehling
PhD candidate
Technical University of Munich, Germany

Omkar Halbe
PhD candidate
Technical University of Munich, Germany

Milan Vrdoljak
Professor
University of Zagreb, Croatia

Matthias Heller
Professor
Technical University of Munich, Germany

Manfred Hajek
Professor
Technical University of Munich, Germany

ABSTRACT

Successful human intervention will be central to any emerging autonomous aerial transport platform, such as personal aerial vehicles (PAV), for the safe conduct of flight. This paper proposes a concept to compensate a partial failure of the autonomous flight guidance by handing over control of the aircraft to a passenger and analyzes the associated human factors. First, a novel waypoint guidance law is designed that generates the desired roll commands for navigation to a designated safe landing spot. Second, two novel guidance display concepts are developed, one for the primary flight display (PFD), and another for the helmet mounted display (HMD), which indicate the desired roll commanded by the guidance law. Third, the guidance law and display concepts are integrated into a high-fidelity, wide field-of-view flight simulation environment and a static mock-up of a conventional helicopter cockpit. Human-in-the-loop experiments were performed with test subjects to analyze the effectiveness of the guidance law and display concepts, and to evaluate piloting performance by non-professional pilots. Various mission task elements were analyzed in these experiments and, in order to intensify workload, a disturbance was included together with a guidance law for commanded roll of PAV. Navigation performance, test subjects' ratings and workload are measured by a combination of objective and subjective analyses. Results indicate that all test subjects were able to reach a close vicinity of the landing spot. Furthermore, the HMD concept shows a lower workload with equal or better navigation performance when compared to the PFD concept.

NOMENCLATURE

x, y, z = position vector in North-East-Down frame, [m]
u = horizontal velocity in local frame, [m/s]
V = total velocity in local frame, [m/s]
χ = track angle with respect to North, [rad]
a_y = lateral acceleration in local frame, [m/s^2]
σ = orientation of the line joining present position to the desired final position, [rad]
$r_\mathrm{h}, r_\mathrm{v}$ = horizontal and vertical components of line of sight joining present and final position, [m]
$\theta = [\varphi\ \theta\ \psi]^T$ = Euler roll angle, [rad]
r = horizontal distance of line of sight joining present and final position, [m]
e = error between w and y, [deg]
w = commanded position, [deg]
y = actual position, [%]
P = precision metric, [%]
t = time, [s]
γ = flight path angle, [deg]
δ_lat = lateral stick input [-90°:90°]
ϕ_c = guidance law for roll angle of PAV [deg]
ϕ_i = input forcing function for roll angle [deg]
ϕ_D2H = commanded roll angle of PAV for mission task element divert to hover [deg]

INTRODUCTION

Personal aerial vehicles (PAVs) are envisioned as the next step towards innovative transport that could combine the freedom of point-to-point personal mobility with the high speeds of air travel. PAVs are defined as self-operating aircraft, capable to be used as flying vehicles by the traveling public (Ref. 1). In case of a system failure that leads to a loss of the flight guidance function, an emergency mode is defined in which a passenger gets partial control of the aircraft. It is assumed that all stabilization functions remain intact and only a final guidance to the safe landing place is required. The goal of this paper is to investigate whether different visual augmentation concepts can be successfully applied to transform a non-piloted PAV to facilitate a passenger to proceed maneuvers it in case of emergency (Ref. 2), in detail a degradation of the Automatic Flight Control System

Presented at the Vertical Flight Society's 76th Annual Forum & Technology Display, Virginia Beach, Virginia, USA, Oct. 6-8, 2020.

(AFCS). There are two key questions involving the passenger of a PAV; first, is there a potential to reduce workload and raise situational awareness offering visual augmentation displays, and second, do such visual augmentation systems differ in handling performance (Ref. 3). However, the broader spectrum of potential PAV occupants are non-pilots; it is therefore considered necessary to use the existing systems of head-down and head-up instrumentation as a basis to develop additional visual augmentation concepts when the intended pilot on an autonomous aircraft is a passenger.

Although very high levels of safety assurance will also be required for the flight control system, the process should also be straightforward for manual flight in addition to a fully autonomous flight. A critical system failure, as like the degradation of the AFCS of the PAV, during flight that leads to a hazardous event (Ref. 1) is therefore used to investigate whether a control strategy for a one axis procedure combined with a visual augmentation display can be successfully applied to transform a PAV to facilitate the passenger to maneuver it in case of this specified emergency use case. However, topics of certification and reliability of PAVs AFCS are taken into account but not discussed within this paper. To achieve this goal, two visual augmentation concepts are considered here: One design is implemented as a head-down cockpit display and one is visualized by a Helmet-Mounted Display (HMD) (Ref. 4).

The present study makes three important contributions. First, it proposes two different augmentation assistance displays (AIDs) to the passenger named as PAV pilot in this paper: a head-down display on the Primary Flight Display (PFD AID) and an HMD AID to explore effects on subjective workload and situational awareness affected by “eyes in the cockpit” and “eyes out of the cockpit” during fulfilling tasks. Second, by displaying a real-time augmentation scheme, it presents a control strategy for managing abnormal situations in a safety-critical environment in which the degree of automation and complexity continues to increase. Third, the PAV pilot workload and performance in fulfillment of flown task is observed by using a specified disturbance signal based on a pilot-model (Ref. 5), which in addition raises subjective workload to create a realistic flight scenario.

This paper is organized as follows. The section problem statement presents the description of the event and assumptions of the study. The methodology for this study is provided afterwards and is followed by a detailed description of the human-in-the-loop simulator experiment and its Mission Task Elements (MTEs) (Ref. 1 and Ref. 6). Subsequently, results from both visual augmentation displays are compared and discussed in regard to limitations of the visualization strategies. Finally, the conclusions and future work are summarized.

PROBLEM STATEMENT

The prospect of a future Urban Air Mobility (UAM) scenario brings up characteristics of the vehicle itself and its mission (Ref. 7). Aircrafts used as PAVs have attributes of an automatic, autonomous, or optionally piloted vehicle. Non-piloted vehicles may be navigated in case of emergency, or if required by a passenger as shown in Figure 1 and Figure 2. The passenger, named as PAV pilot in this paper, may take over control of the non-piloted vehicle in case of a critical system failure. A critical system failure may lead to a hazardous event during flight (Ref. 8). In the event of such an emergency, it is necessary to demonstrate mitigation means in the form of safe landing (Ref. 9).

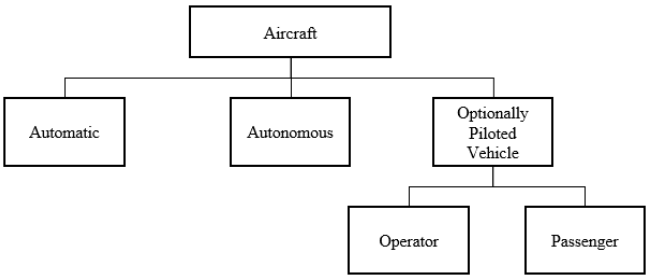

Figure 1. Control classification of aircrafts used in the PAV environment

However, the following assumptions must be made of the environment, where the PAV pilot is observed during the MTEs:

1. The aircraft is equipped with an AFCS (Ref. 10).
2. A degradation of the PAVs’ AFCS is used as a critical system failure, which leads to the hazardous event of the loss of one axis during flight. A continued flight of the non-piloted aircraft is possible if the lost roll axis is controlled by the PAV passenger.
3. All axes of the aircraft are decoupled.
4. During the hazardous event in flight, the aircraft is no longer able to send signals regarding the roll axis to the AFCS but is still able to send the input signal for this axis to the visualization system of the aircraft.
5. The recovery may include the passenger maneuvering the non-piloted vehicle as shown in Figure 2 to a safe hover point. The passengers are therefore instructed before the start of the experiment how to take control of the roll axis by lateral inputs only.

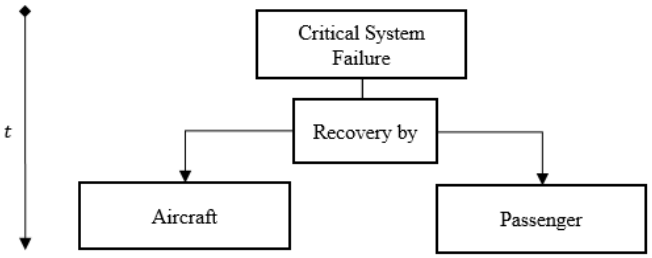

Figure 2. Recovery strategies for a critical system failure of the PAV

The human-in-the-loop simulator experiment explores capabilities of a PAV pilot to react in case of degradation of

AFCS. The cockpit instrument and a Trivisio LCD29 HMD were therefore modified to support the PAV pilot in navigating the aircraft by following a displayed task for the roll axis procedure by lateral inputs of the control element of the aircraft. Modification of both displays in terms of an AID show a real-time waypoint trajectory generation scheme to the PAV pilot on the PFD and HMD.

METHODOLOGY

Focusing on the PAV pilot's workload and augmentation scheme used during AFCS degradation, an aircraft with one axis handling is used. Isolating one axis control during the experiment enables a comparison of workload and effects of different augmentation types examining all PAV pilots involved in the simulator campaign. Therefore, a simulator with a high-fidelity external view creates a realistic scenario during the experiment. The results in this paper arise from the conduct of a simulator campaign in the Rotorcraft Simulation Environment (ROSIE). Further details about ROSIE can be found in Ref. 11.

The simulator campaign was conducted to allow PAV pilots to take over only if they needed control during flight. Therefore, an AFCS degradation that results in the navigation mode being unavailable in roll axis only was simulated. With the loss of stabilization in the roll axis, the PAV pilot had to take over control by using the control device of the aircraft in a lateral axis. Human-in-the-loop experiments are based on flight trials conducted at ROSIE in 2017 and 2018 (Ref. 5 and Ref. 12). The following provides a description of the experimental setup used for execution of flight trials.

Guidance Problem Setup

The simulator campaign was designed to allow PAV pilots to take over only if control is needed during flight. An AFCS degradation that results in the navigation mode being unavailable was simulated. With the loss of stabilization in the roll axis, the PAV pilot had to take over roll axis control by using the cyclic lever of the aircraft in lateral axis.

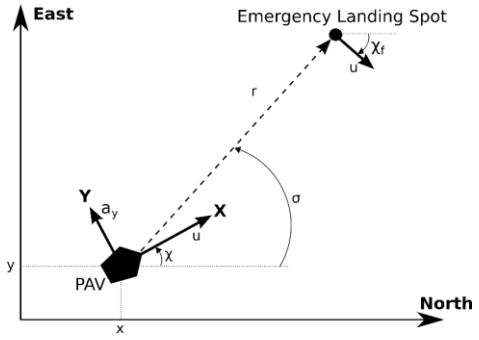

Figure 3. PAV guidance geometry

Consider the scenario depicted in Figure 3. The local reference frame originates at the rotorcraft's center of gravity. The Z-axis (local vertical) points vertically up, the X-axis (local horizontal) is rotated from North about the Z-axis to align with the rotorcraft's heading, and the Y-axis (local lateral) points in port side direction. Sideslip has been neglected. The PAV is in trimmed, level forward flight at the present position (x, y, z) with the velocity vector (u, w, χ). If χ_f denotes the final heading at the landing location, the kinematics using a point mass model are:

$$\dot{\sigma} = \frac{u}{r}\sin(\chi - \sigma) \tag{1}$$

$$\dot{\chi} = \frac{a_y}{u} \tag{2}$$

Where, σ is the angle and r is the length of the horizontal line of sight from the present position to the landing location with respect to North, and a_y is the lateral acceleration. The guidance objective is to generate the lateral acceleration necessary to steer the PAV towards the landing spot with the desired final heading in real-time. The necessary conditions to reach the final position at χ_f are:

- $\chi \to \chi_f$, and
- $\sigma \to \chi_f$

Lateral Acceleration Guidance Law

To satisfy the necessary conditions, the state vector is defined as $\boldsymbol{x} \equiv [e_\sigma\ e_\chi]^T$, where $e_\sigma = \chi - \chi_f$ and $e_\sigma = \sigma - \sigma_f$. The control variable is simply the lateral acceleration, $\boldsymbol{u} \equiv [a_y]^T$. The problem can be formulated as nonlinear quadratic regulator. The State-dependent Riccati Equation (SDRE) technique (Ref. 13) is ideally suited for a nonlinear control-affine system of Eqns. (1)-(2) $\dot{\boldsymbol{x}} = \boldsymbol{F}(\boldsymbol{x}) + \boldsymbol{B}(\boldsymbol{x})\boldsymbol{u}$. The resulting algebraic Riccati equation is solved analytically to obtain the nonlinear feedback control law for the lateral acceleration. In the first step, the system of Eqns. (1)-(2) is parameterized for e_σ and e_χ, and written in nonlinear SDC form $\dot{\boldsymbol{x}} = \boldsymbol{A}(\boldsymbol{x})\boldsymbol{x} + \boldsymbol{B}(\boldsymbol{x})\boldsymbol{u}$, as follows:

$$\begin{bmatrix} \dot{e}_\sigma \\ \dot{e}_\chi \end{bmatrix} = \begin{bmatrix} -\frac{u\sin(e_\chi - e_\sigma)}{r(e_\chi - e_\sigma)} & \frac{u\sin(e_\chi - e_\sigma)}{r(e_\chi - e_\sigma)} \\ 0 & 0 \end{bmatrix} \begin{bmatrix} e_\sigma \\ e_\chi \end{bmatrix} + \begin{bmatrix} 0 \\ \frac{1}{u} \end{bmatrix} a_y \tag{3}$$

The SDRE necessary conditions, as recalled from Ref. 13 are:

1) $\{\boldsymbol{A}, \boldsymbol{B}\}$ is controllable.

2) $\boldsymbol{F}(\boldsymbol{x})$ is continuously differentiable.

3) $\boldsymbol{F}(\boldsymbol{0}) = \boldsymbol{0}$. To verify the first condition, the rank of the controllability matrix $\boldsymbol{M}(\boldsymbol{x})$. These conditions are readily shown to be satisfied (Ref. 10).

In the next step, the following infinite horizon quadratic cost function must be minimized:

$$J = \frac{1}{2}\int_{t_0}^{\infty} [\mathbf{x}^{\mathrm{T}}\mathbf{Q}(\mathbf{x})\mathbf{x} + \mathbf{u}^{\mathrm{T}}\mathbf{R}(\mathbf{x})\mathbf{u}] \tag{4}$$

The weighting elements for the present problem are chosen as $\boldsymbol{Q}(\boldsymbol{x}) = \mathrm{diag}(q_1^2, q_2^2)$ and $R = 1$. The feedback control law is obtained by solving the algebraic Riccati equation for the unique, symmetric and positive-definite matrix $\boldsymbol{P}(\boldsymbol{x})$ according to Ref. 13.

$$\mathbf{A}^{\mathbf{T}}(\mathbf{x})\mathbf{P}(\mathbf{x}) + \mathbf{P}(\mathbf{x})\mathbf{A}(\mathbf{x}) - \mathbf{P}(\mathbf{x})\mathbf{B}(\mathbf{x})\mathbf{R}^{-1}(\mathbf{x})\mathbf{B}^{\mathbf{T}}(\mathbf{x})\mathbf{P}(\mathbf{x}) + \mathbf{Q}(\mathbf{x}) = \mathbf{0} \tag{5}$$

where, $\mathbf{P} = \begin{bmatrix} p_{11} & p_{12} \\ p_{12} & p_{22} \end{bmatrix}$. Upon substitution from Eqn. (3) followed by algebraic manipulations, one obtains the analytical solution of the elements of $\boldsymbol{P}(\boldsymbol{x})$. The lateral acceleration control law is obtained from the solution of the algebraic Riccati Eqn. (5) as:

$$a_y^* = -R^{-1}\mathbf{B}(\mathbf{x})^{\mathrm{T}}\mathbf{P}(\mathbf{x})\mathbf{x} \tag{6}$$

which yields:

$$a_y^* = -\frac{p_{12}(\sigma - \chi_f)}{u} - \frac{p_{22}(\chi - \chi_f)}{u} \tag{7}$$

where,

$$p_{22} = -\xi u^2 \pm u\sqrt{\xi^2 u^2 + 2\xi u\sqrt{q_1^2 + q_2^2} + q_2^2}$$

$$p_{12} = u\sqrt{q_1^2 + q_2^2} - p_{22}$$

$$\xi = \frac{u\sin(e_\chi - e_\sigma)}{r(e_\chi - e_\sigma)}$$

Eqns. (6)-(7) are used to generate the necessary lateral acceleration in forward flight to achieve the desired final position and heading simultaneously. Assuming small sideslip in forward flight, the required change in roll angle to achieve the lateral acceleration is generated as follows:

$$\Delta\phi_c \approx \arctan\left(\frac{a_y^*}{g}\right) \tag{8}$$

The commanded roll angle for display is obtained by adding the roll change to its trim value, as follows:

$$\phi_c = \phi_{\mathrm{trim}} + \Delta\phi_c \tag{9}$$

Guidance Display Concepts

For the assessment of the manually flown tasks in roll axis based on Ref. 6, a guidance symbology was displayed on the PFD or HMD to assist the PAV pilots in fulfilling the different tasks. The guidance symbology includes the roll axis guidance law (Ref. 14) and a distortion signal enables measurements on PAV pilot performance and to carry out subjective workload. It is intended to display the actual position of the aircraft y as well as the reference, commanded position w in a simplified and conventional augmentation type to the PAV pilot. Important information of the error e is given to the pilot visually. Bearing and distance to the hover point, decrementing from 90° down to 0° and 10 NM to 0 NM are indicated to the left and right side of the modified Attitude Direction Indicator (ADI) in a numeric readout section. To follow the desired trajectory, the PAV pilots were required to maintain the error $e = 0$. Both PFD and HMD ADI schematic concepts are shown in Figure 4 and Figure 5.

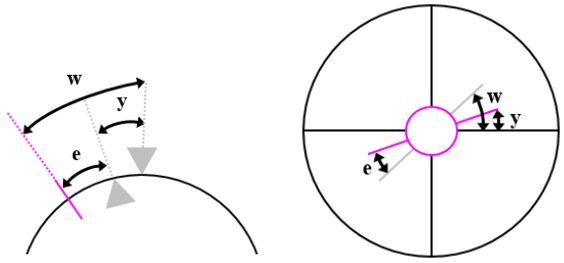

Figure 4. Schematic modified PFD (left) and HMD (right) ADI

Both modified ADIs, presented on PFD and HMD, behave in the same way regarding motion speed and integrated values e, w, y.
Value w represents the commanded position of the PAV in roll axis in degrees shown as a horizontal line. Actual roll is shown by value y in degrees shown as a horizontal line. Both lines w, y are rotating around the center point of ADI. Value e represents the error between w and y, which is mainly used for post flight analysis. Furthermore, the value e is also important to the pilot – his actions are guided by this value trying to set $e = 0$. Above that value, e is used in the objective analysis as a measure of precision of each flight.

Integration for Rotorcraft Simulation Environment

The experiments with human-in-the-loop simulations were executed in ROSIE (Ref. 11), a realistic flight environment, located at the Institute of Helicopter Technology, TUM Department of Mechanical Engineering, Technical University of Munich. The human-in-the-loop fixed-based simulator is equipped with a high-fidelity visual system. It utilizes a nonlinear flight model with the blade aerodynamic model based on the blade element/ momentum theory with simple analytical downwash models and rigid blades.
Used augmentation assistance systems implemented in the head down and a modified Trivisio LCD-29 helmet mounted display (Ref. 15) are arranged as follows: PFD AID is displayed on the central multifunctional display of the cockpit while HMD AID is visualized by a helmet mounted display with see-through capabilities, both as shown in Figure 5.

Figure 5. PAV pilots using PFD (left image) and HMD (right image) during MTEs

The PAV pilots have to align visualized actual to desired value of real-time waypoint trajectory scheme by lateral cyclic stick inputs regarding subjective workload and

following precision using PFD AID and HMD AID as shown in Figure 6. Figure 6 shows HMD AID with the see-through capability to the outside scenery. During the human-in-the-loop experiment, PAV pilots see the outside scenery while wearing the HMD using the HMD AID. The black background of the HMD as shown in Figure 6 is therefore transparent during the experiment.

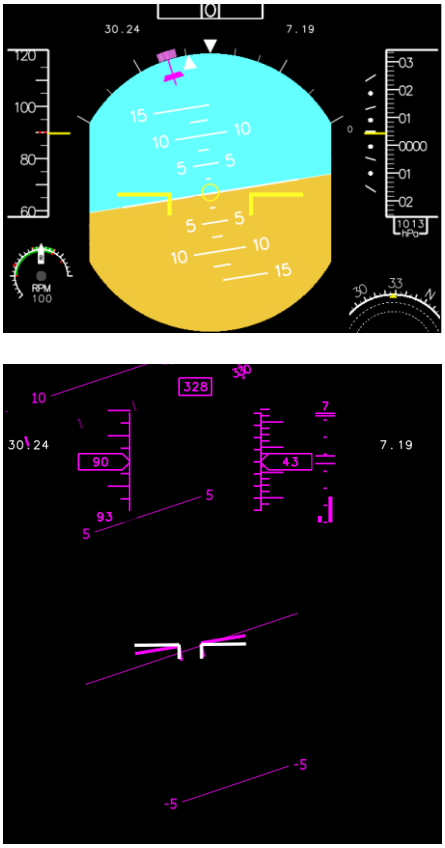

Figure 6. PFD (upper image) and HMD (lower image) AID during MTE 2

PFD AID and HMD AID both consist of two parts: A modified ADI symbology and two numeric values. The modified ADI is displayed in the PFD in the upper part of the central field of regard to the PFD including a commanded and an actual roll angle in degrees displayed in magenta and white. Looking at the modified HMD ADI, the commanded (white) and actual (magenta) role angle in degrees is displayed in a pitch stabilized ADI.

The second part of the PFD AID and HMD AID consists of two numeric values displayed to the left and right side of the modified PFD ADI and HMD ADI. Regarding PFD AID and HMD AID, both augmentation designs were designed similar in arrangement of the displaying values. Therefore, two numeric values are displayed at the upper edges of the modified ADIs. The numeric value, which is arranged on the right side, shows the distance to the safe hover point in nautical miles (NM) counting downwards from 10 NM (start of experiment) to 0 NM (end of experiment). The numeric value to the left side of the modified ADIs displays the bearing in degrees to the safe hover point. The value is also decreasing from 90° (start of experiment) to 0° (end of experiment) like the value on the right side.

DESIGN OF HUMAN-IN-THE-LOOP EXPERIMENT

Purpose of experiments

The simulator campaign focused on the assessment of subjective workload and manual control input performance of 30 PAV pilots participating in sum in the experiment, each named with an ID (PIDs) to fulfill two MTEs (Ref. 14 and Ref. 16). Two different guidance display concepts were therefore offered to the PAV pilots on the PFD and the HMD to analyze preferences and effects of offered AID on head-down and head-up instruments. Workload and precision had been investigated for each PAV pilot and all PAV pilots in common regarding the effects and trends of AID acceptance and possible improvements of displayed values.

Test subjects

The flight test campaign involved a total of 30 test subjects ranging in age from 21 to 67 years including 6 female and 24 male participants. All of them were non-professional pilots. However, all PAV pilots were commonly described by their prior flight experience in real world and simulator (Sim) experience with fixed wing and rotary wing aircrafts as shown in Table 1 with mean values and standard deviations in brackets.

Table 1. PAV pilots of human-in-the-loop experiment including experiences

No. of PID	Age	A/C flown Front Seat	H/C Sim flown Front Seat	H/C Sim flown using Glass Cockp.	H/C Sim flown using HUD	H/C Sim flown using HMD
30	30.7y (9.4y)	0.2h (0.9h)	3.0h (5.6h)	2.1h (3.1h)	0.2h (0.9h)	0.8h (0.9h)

In addition to the visual augmentation experience, all PAV pilots were asked about their experience stated in flight hours in simulator flying, flying within a glass cockpit (multifunctional display showing PFD), using a Head-Up Display (HUD), and an HMD in terms of being able to achieve the task at least at an adequate level. The order of tasks was randomized over all PAV pilots to face learning effects and simulator sickness. Simulator sickness (SSQ) was regarded by using Ref. 17. Almost none of the PAV pilots showed moderate or severe effects of simulator sickness as shown in Figure 7 after finishing the experiment, having completed all MTEs successfully. The numbers of flown MTEs were limited as detailed in IV to avoid fatigue effects and discomfort regarding subjective workload and flight performance.

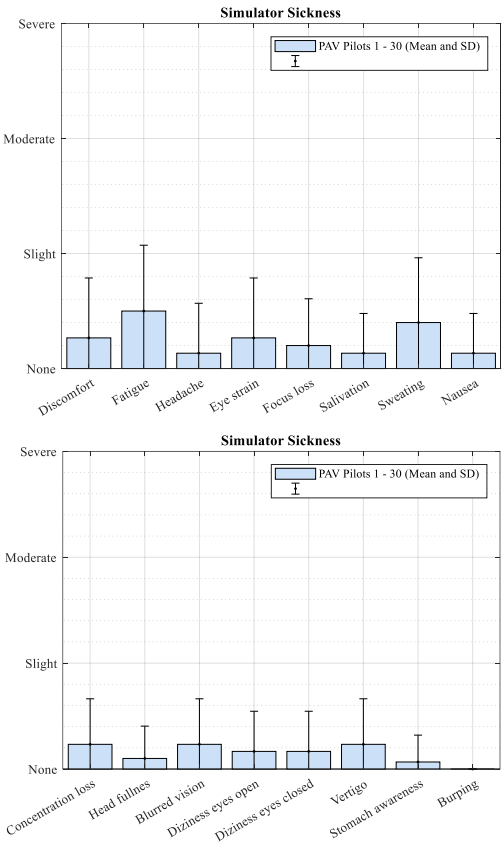

Figure 7. Simulator sickness evaluation of all participating PAV pilots

Mission Task Elements

The PAV communicating mission was broken down to several MTEs (Ref. 16). Regarding the MTEs executed in this study, each PAV pilot was able to generate inputs by lateral axis using the cyclic control of the aircraft only. All other axes excepting the roll axis of the aircraft were stabilized by the AFCS.

The MTEs1 as shown in Table 3, were conducted as reference flights to the different display formats and for getting the PAV pilots familiar with the aircraft environment. To fulfill the MTEs1, the PAV pilot had to keep the aircraft stable in a direction with a roll angle of 0° using cyclic control in lateral axis only as input. Regarding MTEs1 with visual cues only as the initial stage of research, PAV pilots had to fulfill the task by looking out of the cockpit, viewing the outside scenery and using visual cues only. In the following two MTEs1, the PAV pilots were offered the use of conventional guidance symbology of a PFD ADI and an HMD ADI.

Following both MTEs2, the PAV pilots had to follow the displayed roll guidance by using cyclic control in the lateral axis only just like during the MTEs1. Both MTEs2, were executed in the same setting as during MTEs1: All maneuvers began with a stable, straight, and level cruise flight at a forward speed of 80 kts, at a height of 1,500 ft above ground level (AGL), and 10 NM away and 90° bearing from the desired hover position. Each maneuver began 10 sec. after the test instructor announced the MTE to the PAV pilot with the command “Start”. The maneuver was completed once 150 sec. of flight was performed as shown in Figure 14. In accordance with the beginning of the experiment, the end of the task was announced to the PAV pilot after 150 sec. of flight by the test instructor with the command “Stop”. Simulation was stopped simultaneously. During both MTEs2, the PAV pilots benefited from using a modified conventional PFD ADI only and a modified HMD ADI only. An overview of all MTEs connected to AIDs and its order of execution (OE) is shown in Table 2.

Table 2. Test setup of simulator campaign

MTE No.	MTE	AID	OE PID 1-15	OE PID 16–30
1	Straight and level cruise	Visual cues only	1	1
1	Straight and level cruise	Conventional PFD only	2	3
1	Straight and level cruise	Conventional HMD only	3	2
2	Divert to hover point	Modified PFD only	4	5
2	Divert to hover point	Modified HMD only	5	4

The test setup strictly proceeded with each PAV pilot in the same manner. Therefore, a specific experimental design was implemented. The experimental design consisted of a detailed test plan as shown in Table 3 including a briefing before all MTEs were executed and debriefing after fulfilling all MTEs. Debriefing consisted of three questionnaires focusing on simulator sickness, display concepts, and a biographic questionnaire.

Table 3. Experimental design of human-in-the-loop experiment

Test Proceeding	Time Duration (min.)	Test Proceeding Element
Briefing	10	Introduction to ROSIE
	10	Introduction to MTEs
MTE 1	5	Execution of MTE
	2	Short Break
MTE 1	5	Execution of MTE
	2	Short Break
MTE 1	5	Execution of MTE
	2	Short Break
MTE 2	5	Execution of MTE
	2	Short Break
MTE 2	5	Execution of MTE
Briefing	10	Questionnaire Simulator Sickness
	2	Short Break
	10	Questionnaire Display Concepts
	10	Questionnaire Biography

Elements of Objective Analysis

Beside the subjective assessment of the workload, experiments were also prepared for the objective analysis of proceeded PAV pilot flights according to the recorded values from the ROSIE flight simulator. This preliminary analysis was introduced to evaluate how precise PAV pilots were able to fulfill presented MTEs in a simulated aircraft environment. The focus of this analysis was set to MTEs2, where the guidance algorithm, as detailed in Section III, could also be tested. However, all MTEs1 were considered for further discussions within the questionnaires that were filled out during the debriefing. The idea of putting a disturbance signal on top of the displayed guidance signal was to intensify the subjective workload of each PAV pilot. The distortion signal given with Eqn. (10) was presented together with the guidance signal on the modified PFD ADI and HMD ADI, so that the commanded roll for MTE divert to hover would be

$$\phi_{D2H} = \phi_c + \phi_i \tag{10}$$

where ϕ_i presents this disturbance, also called input forcing function. The definition of this input forcing function originates from the analysis of the pilot model: It is used in Ref. 5 and Ref. 12 as an input signal, as a forcing function that could enable estimations of the pilot model. The signal defining the input forcing function is pseudo-stochastic. It is defined in the same manner for all flights in the conducted experiment. However, it would appear to be stochastic to the PAV pilots: The distortion signal is generated as a sum of sinusoids with different amplitudes, frequencies and phase shifts, and a prescribed variance, according to Ref. 5. The commanded signal defined with Eqn. (10), including the guidance and the distortion signal is displayed to the PAV pilot within the PFD AID and the HMD AID during MTEs2.

RESULTS AND DISCUSSION

Overall, the results measuring PAV pilots' subjective workloads and precision in fulfilling MTEs2 by using the AIDs showed a significance ($Pr = .8, N = 30, \alpha = .05, r = 0.48$) of lower subjective workload using HMD AID versus PFD AID with a similar precise handling being measured using HMD AID compared to PFD AID. However, the subjective workload increased as expected from MTEs1 to MTEs2.

Assessment of Subjective Workload

Facing the question of whether a PAV pilot can assist the PAV in navigating to a safe hover point with the help of displayed AIDs on the PFD and HMD, the experiments focused on subjective workload and precise navigation using different AID systems.

The first objective of this study was to examine PAV pilots' subjective workloads during two different MTEs. Beside the two different MTEs with an increasing complexity of flight, three different AIDs considered effects of the eyes out of the cockpit (using visual cues or the HMD only), and effects of eyes inside the cockpit (using the PFD only). As starting point for this investigation, all PAV pilots undertook the flight trial using only the outside world visual cues, PFD only, and HMD only to familiarize themselves with the simulation environment (MTEs1). In the next step, PAV pilots benefited from using a modified PFD ADI and HMD ADI to fulfill the MTEs2. All PAV pilots were asked instantaneously after fulfilling each single flight on their subjective workload. The subjective workload was specified and measured within a Likert scale inspired by the Bedford workload rating scale (Ref. 16). However, the Bedford workload rating scale is used for professional pilots only; the subjective workload analysis in this paper may show a general tendency. The following values were therefore used: 0 – insignificant workload, 1– very low workload, 2–low workload, 3–high workload, 4– very high workload.

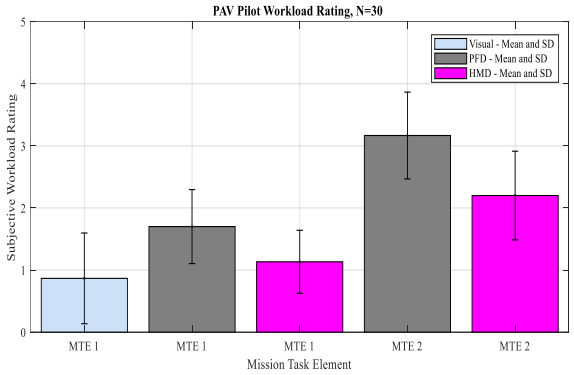

Figure 8. PAV pilots' subjective workload using different augmentation types (N=30)

By looking at the results from Figure 8, the increase of the subjective workload from MTEs1 to MTEs2 is in accordance with an increasing complexity of the flown tasks from MTEs1 to MTEs2. The trend of a lower subjective workload using the HMD versus the PFD over all conducted flights may arise from 23 out of 30 PAV pilots, who reported that they were able to have the outside scenery in sight using the HMD versus the PFD. They reported a benefit from the see-through capability during quiescent periods of flight when guidance command, lasting some seconds, was not felt intensively. Almost all participants stated not being able to have the outside scenery in view while using the PFD during fulfilling MTEs2. It may be assumed, that the eyes out-of-the-cockpit effect led to a lower workload of the PAV pilots who had the whole scenery, and finally the safe hover point in sight. However, the wearing comfort of the HMD was stated acceptable by all PAV pilots. Moreover, the presentation of the head-down instrumentation and the head-up instrumentation were both rated acceptable facing the distances between the PAV pilots' eye points and the center of the displays.

Leading from the subjective workload to the preference of the display type, PAV pilots were asked about their preferences of the display type after fulfilling all MTEs as shown in Figure 9.

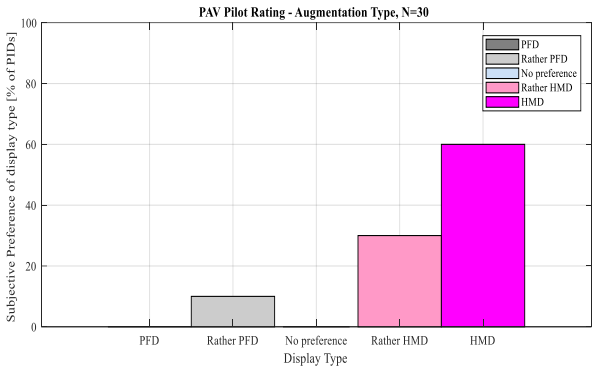

Figure 9. PAV pilots' preferences of augmentation display types (N=30)

Almost all PAV pilots chose either HMD or HMD. Although all conducted flights were operated in a normal cruise altitude for PAVs, and a good weather environment (GVE), only 2 out of 30 PAV pilots were able to have the urban environment in sight during the flights while using the PFD. In contrast, 28 of 30 PAV pilots stated that they had the urban environment in sight while using the HMD. In detail regarding MTEs2, it may be assumed that the PAV pilots were not able to estimate at which time during the flight and in which form of intensity the guidance roll command would be displayed and therefore requested inputs from the PAV pilot. It could be expected that PAV pilots were not able to raise their head and therefore were not able to incorporate the outside scenery to their field of regard while using the PFD, because they always had to expect a new guidance command. This was unlike when the PAV pilots were offered to use the HMD. PAV pilots had the capability to shift focus between displayed values and the outside scenery and therefore had both in sight: the outside scenery and the displayed values. It may help the PAV pilots that the focus of HMD is set to infinite, which allowed the PAV pilots to at least detect the guidance value changes while looking at the outside scenery through the HMD. However, the Situational Awareness (SA) may be higher while using the HMD than the PFD. SA was queried in general to with PAV pilots since the SA rating is used for professional pilots only. This may be included in further experiments in this environment.

In addition, the PAV pilots were asked in detail about the ADI augmentation formats as shown in Figure 10 displayed on the PFD and HMD with the question of how intuitively conventional aircraft displays may appear to non-professional pilots.

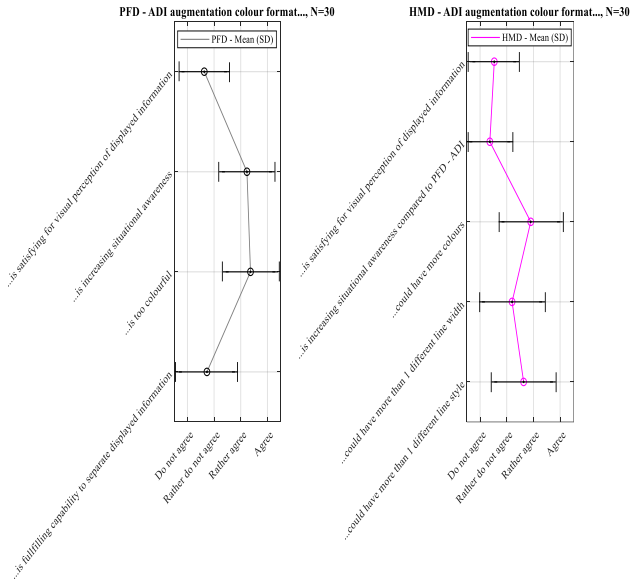

Figure 10. Situational Awareness within PFD ADI and HMD ADI augmentation color formats (N=30)

In general, all PAV pilots were able to fly with the displayed conventional ADIs presented on the PFD and on the HMD. However, both PFD and HMD ADI may have to be adapted due to the fact that a PAV pilot is usually not familiar with conventional flight instrumentation: Most of the PAV pilots noted, that while the PFD ADI showed too much information to the PAV pilot, they missed an artificial prominent horizon within the HMD displayed symbology. Almost all PAV pilots intuitively assumed that they had to keep the symbol of the aircraft itself above or on the horizontal 0° line of the ADIs during flight. Although the PFD ADI and HMD ADI increased the general SA of most of the PAV pilots, it may be discussed how the PFD ADI could be simplified, and if a more prominent horizon should be implemented with the HMD AID to further enhance the general SA. All PAV pilots stated that the PFD ADI including the AID offers a more precise handling capability than the HMD ADI including the AID during MTEs2. This may lead to the discussion of whether PAV pilots would prefer a more detailed HMD AID by adapting the actual HMD AID - different line styles and widths could offer the PAV pilots both roll angles of the HMD ADI, commanded and actual, in sight at the same time as the PFD AID offers. Within deeper discussions with the PAV pilots, it turned out that even a color behavior of the HMD AID may help. As an example, 4 PAV pilots independently stated to change the ADI to green color by the time the PAV pilot reaches the exact roll angle. In contrast, the PAV pilots mentioned that the symbology concept of the PFD AID is satisfying regarding the symbols used and their behavior. Overall, almost none of the PAV pilots referred to the displayed numeric values during flight. PAV pilots reported not being able to connect the numeric values to the presented scenery. It will be further investigated, if they are needed, by implementing them into a symbol concept to improve the presentation of these values.

Objective Analysis

Beside the assessment of the subjective workload, this section focuses on the ability of PAV pilots to follow the displayed commanded roll angle in precision and therefore to fulfill the MTEs. Within MTEs2, each PAV pilot had to align the aircraft to a predefined route as shown in Figure 11, starting with the flight path shifted by 90° from a safe hover point. Regarding the analysis in flight precision, the error in roll angle of each PAV pilot was set to relevant, which is shown exemplary in Figure 12: the displayed recording in Figure 12 shows the relevant values of MTEs2 as described earlier in this paper.

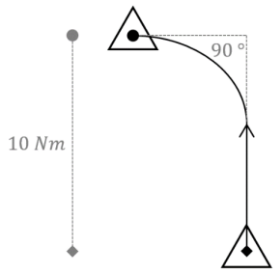

Figure 11. Top view routing of MTE 2

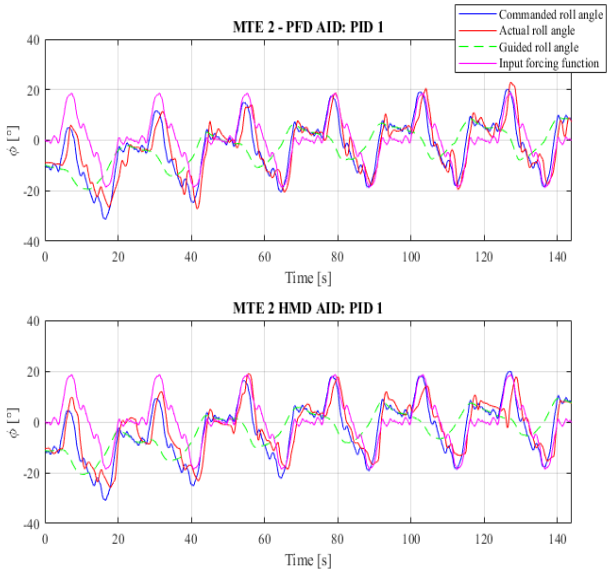

Figure 12. Actual roll versus commanded roll signal of PAV pilot 1 during the MTEs2

The flight-path control was performed satisfactorily by all PAV pilots using PFD and HMD as shown in Figure 13. It may be assumed that all PAV pilots succeeded in fulfilling the MTEs by also reaching the safe hover point in the end. Since none of the PAV pilots were professional pilots, it could be stated that a reduced control complexity regarding expected inputs from the PAV pilots enhanced fulfillment of the MTEs: In these cases, all other axes except the roll axis of the aircraft were stabilized by the AFCS and all axes were completely decoupled, so the PAV pilots had to set inputs to the PAV using the cyclic control of the PAV only in one axis direction.

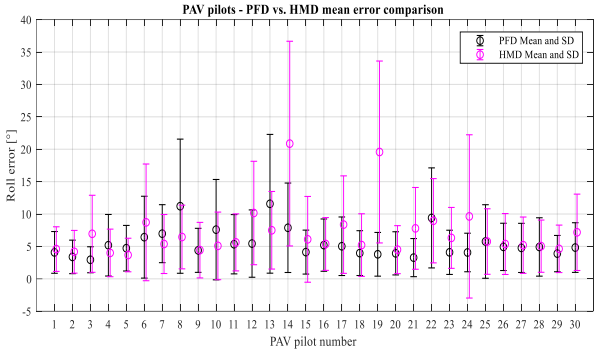

Figure 13. Comparison of values for mean error between the commanded and actual roll angle for PFD versus HMD during MTEs2 (N=30)

However, 3 out of 30 PAV pilots showed a higher mean error compared to the rest of the test persons during MTEs2 as seen in Figure 13. PAV pilot numbers 14 and 24 were in parallel, two out of the three PAV pilots preferred the PFD as shown in Figure 9. It may be discussed if these two PAV pilots would have needed more time to get familiar with the HMD. PAV pilot number 19, the oldest participant in this experiment at 67 years, stated his subjective workload while using the HMD was just as high when using the PFD.

CONCLUSIONS

This paper described an assessment of 30 passengers, named as PAV pilots, during needed takeover of control of a non-piloted PAV while benefiting from two different visual augmentation assistance systems during different MTEs. To overcome the challenge for a PAV pilot to assist the PAV in case of its degradation of the AFCS, two augmentation assistance displays (AIDs) were designed and integrated into the Rotorcraft Simulation Environment. With a focus on decreasing the workload and increasing the precision in fulfillment of the MTEs by the PAV pilots, a modified ADI was provided on a primary flight display (PFD) and on a helmet mounted display (HMD) with see-through capabilities. Investigations offered a lower subjective workload to the PAV pilots by benefiting from “the eyes out of the cockpit” effect while using the HMD compared to the PFD. Moreover, the objective results showed a tendency to higher precision flights using the modified PFD symbology than the modified HMD symbology. Therefore, the PAV pilots had to operate the PAV to a safe hover point in case of an in-flight emergency using the cyclic control of the PAV in one axis direction. Both of the modified ADIs, displayed on PFD and HMD, included a guidance law and a distortion signal, derived from a pilot model to carry out subjective workloads and to compare the flights of the participating PAV pilots. The main conclusions drawn from the human-in-the-loop experiments were as follows:

1) A physiological and perceptual acceptance of both augmentation assistance displays, PFD and HMD, was shown by all tested PAV pilots. Both display concepts benefited from each other. While the PFD AID had a higher precision rate, the HMD AID profited from decreasing subjective workload. However, the HMD AID may profit from an

augmentation concept that offers a larger filigree symbology displayed for a higher precision rate. On the other hand, the PFD AID may profit from a reduction of displayed values so not to overstrain the PAV pilots.

2) Almost all PAV pilots chose either HMD or HMD after having fulfilled the MTEs. This may be due to the "eyes out of the cockpit" effect from the HMD offering the PAV pilots both outside scenery and the displayed values in sight during the flights.

3) All PAV pilots fulfilled the given MTEs demanding inputs from the PAV pilot by single axis inputs to the roll axis with acceptable effort and precision. In general, the precision in fulfilling the MTEs2 was higher during the use of the PFD than the HMD. However, taking prior investigations focused on the control of the pitch axis (Ref. 5) of the PAV into account, the experiments might be extended to coupled axes in-flight tasks regarding lateral and longitudinal inputs.

With a view to the AFCS, it could be discussed what type of controller would be needed to allow the PAV pilot to assist the PAV in case of emergency in control with respect to subjective workload and precision in flight. The modified PFD and HMD ADI designs might also have to be adapted to the fact that passengers of a PAV are not always familiar with conventional flight instrumentation.

Author contact:
Tim Mehling Tim.Mehling@tum.de
Omkar Halbe Omkar.Halbe@tum.de
Matthias Heller Matthias.Heller@tum.de
Milan Vrdoljak Milan.Vrdoljak@fsb.hr
Manfred Hajek Hajek@tum.de

ACKNOWLEDGMENTS

The work reported in this paper is funded by the Institute of Helicopter Technology at the Technical University of Munich. The authors would like to thank all of those who have participated in the simulation trials reported in this paper for their contribution to the research. Special thanks go to the members of the University of Zagreb at the faculty of Mechanical Engineering and Naval Architecture, the members of the Institute of Flight Systems Dynamics, and the members of the Institute of Helicopter Technology from the Technical University of Munich for participating in deep discussions on the topic of Urban Air Mobility.

REFERENCES

1. Geluardi, S., Venrooij, J., Olivari, M., Bülthoff, H. H., and Pollini, L., "Transforming Civil Helicopters into Personal Aerial Vehicles: Modeling, Control, and Validation," Journal of Guidance, Control, and Dynamics; Vol. 40, No. 10, 2017, pp. 2481–2495. doi: 10.2514/1.G002605.

2. Lu, L., Jump, M., White, M., and Perfect, P., "Development of Occupant-Preferred Landing Profiles for Personal Aerial Vehicles," Journal of Guidance, Control, and Dynamics; Vol. 39, No. 8, 2016, pp. 1805–1819. doi: 10.2514/1.G001608.

3. Perfect, P., Jump, M., and White, M. D., "Handling Qualities Requirements for Future Personal Aerial Vehicles," Journal of Guidance, Control, and Dynamics; Vol. 38, No. 12, 2015, ppCl. 2386–2398. doi: 10.2514/1.G001073.

4. Harding, T. H., Rash, C. E., McLean, W. E., and Martin, J. S., "The impact of human factors, crashworthiness and optical performance design requirements on helmet-mounted display development from the 1970s to the present," Display Technologies and Applications for Defense, Security, and Avionics IX; and Head- and Helmet-Mounted Displays XX, SPIE, 2015, 94700U.

5. Vrdoljak, M., Viertler, F., Hajek, M., and Heller, M., "Helicopter Pilot Model for Pitch Attitude Tracking Task," Advances in Aerospace Guidance, Navigation and Control, edited by B. Dołęga, et al., Vol. 3144, Springer International PU, 2017, pp. 225–239.

6. "Aeronautical Design Standard Performance Specification Handling Qualities Requirements for Military Rotorcraft," U.S. Army Aviation and Missile Command Aviation Engineering Directorate, ADS-33E-PRF, Redstone Arsenal, AL, 2000.

7. Cornes, O., "Basic design limitations for urban electric VTOL aircraft," Proceedings of the 75th Annual Forum, Philadelphia, 2019.

8. ARP4761: Guidelines and Methods for Conducting the Safety Assessment Process on Civil Airborne Systems and Equipment-SAEInternational, https://www.sae.org/standards/content/arp4761/, [retrieved 26 April 2019].

9. Cacciavillani, E., and Ielmini, F., "Numerical study and optimization of a novel architecture of Vertiport and Vertistop for Urban Air Mobility," Proceedings of the 75th Annual Forum, Philadelphia, 2019.

10. Halbe, O., Spiess, S., and Hajek, M., "Rotorcraft Guidance Laws and Flight Control Design for Automatic Tracking of Constrained Trajectories", AIAA Guidance, Navigation, and Control Conference, AIAA SciTech Forum, Kissimmee, Florida, 8–12 January 2018. doi: 10.2514/6.2018-1343

11. Viertler, F., Hajek, M., "Requirements and Design Challenges in Rotorcraft Flight Simulations for Research Applications," AIAA SciTech - Modeling and Simulation Technologies Conference, Kissimmee, Florida, USA, 2015.

12. Vrdoljak, M., Halbe, O., Mehling, T., Hajek, M., "Simulator Experiments for Modeling Helicopter Pilot in Roll Tracking Task," AIAA SciTech - Modeling and Simulation Technologies Conference, Orlando, Florida,

USA, 2020.

13. Cloutier, J. R., and Stansbery, D. T., "The Capabilities and Art of State-Dependent Riccati Equation-Based Design", Proceedings of the American Control Conference, Anchorage, AK, May 8-10, 2002. doi: 10.1109/ACC.2002.1024785

14. Hess, R. A., "Modeling Human Pilot Adaptation to Flight Control Anomalies and Changing Task Demands," Journal of Guidance, Control, and Dynamics; Vol. 39, No. 3, 2016, pp. 655–666. doi: 10.2514/1.G001303.

15. Viertler, F., Bengler, K., Hajek, M.," Visual Augmentation for Rotorcraft Pilots in Degraded Visual Environment," http://nbn-resolving.de/urn/resolver.pl?urn:nbn:de:bvb:91-diss-20170421-1335668-1-9, [retrieved 16 October 2019]. TUM Technical University of Munich, Munich, Germany, 2017.

16. Perfect, P., Jump, M., and White, M. D., "Methods to Assess the Handling Qualities Requirements for Personal Aerial Vehicles," Journal of Guidance, Control, and Dynamics; Vol. 38, No. 11, 2015, pp. 2161–2172. doi: 10.2514/1.G000862.

17. Kennedy, R. S., Lane, N. E., Berbaum, K. S., and Lilienthal, M. G., "Simulator Sickness Questionnaire: An Enhanced Method for Quantifying Simulator Sickness," The International Journal of Aviation Psychology; Vol. 3, No. 3, 1993, pp. 203–220. doi: 10.1207/s15327108ijap0303_3.